IARJSET

ISSN (O) 2393-8021, ISSN (P) 2394-1588

International Advanced Research Journal in Science, Engineering and Technology

Impact Factor 8.066 ⁜ Peer-reviewed & Refereed journal ⁜ Vol. 11, Issue 8, August 2024

DOI: 10.17148/IARJSET.2024.11842

Removal of Anionic Dye from Aqueous Solution Using Treated Laterite Adsorbent: Response Surface Methodology Approach

Madhusudhana Reddy Mule[1*], Anila Pulikam[1], G.V.S Sarma[2], K.V. Ramesh[2]

Department of Chemical Engineering, RGUKT Nuzvid, Nuzvid-521202, India[1]

Department of Chemical Engineering, Andhra University, Visakhapatnam-530003, India[2]

Abstract: This study investigates the removal of Congo red (CR) dye from aqueous solution using treated laterite (TL) as a low-cost adsorbent. The effects of pH, contact time, initial dye concentration, adsorbent dosage, and temperature on adsorption efficiency were evaluated. Equilibrium was established within 90 minutes, with negligible temperature effects observed. Response Surface Methodology (RSM) with Central Composite Design (CCD) was employed to optimize three adsorption parameters: pH (4–7), initial dye concentration (10–50 mg/L), and adsorbent dosage (200–1500 mg). ANOVA analysis revealed that all three factors were statistically significant ($p < 0.001$), but initial concentration exerted the strongest influence (F-value = 256.94). Significant two-way interactions were identified between pH and dosage ($p = 0.000$, $F = 32.36$) and pH and concentration ($p = 0.015$, $F = 8.64$). The quadratic model demonstrated excellent fit with $R^2 = 0.9707$ and adjusted $R^2 = 0.9442$. Optimal conditions for maximum dye removal were determined to be pH 4.8, an initial dye concentration of 52 mg/L, and an adsorbent dosage of 850 mg. These findings demonstrate that treated laterite is an effective, sustainable adsorbent for the removal of anionic dyes from textile wastewater.

Keywords: Congo red dye; Treated laterite; Adsorption; Response surface methodology; Central composite design; ANOVA; Wastewater treatment.

1. INTRODUCTION

The textile industry represents one of the largest global manufacturing sectors, contributing significantly to employment generation and economic development [1]. However, this industry is concurrently identified as a major contributor to environmental pollution, particularly water contamination resulting from dyeing operations [2]. The discharge of synthetic dyes into aquatic ecosystems poses severe ecological risks, including disruption of photosynthetic processes in aquatic plants and potential carcinogenic and mutagenic effects on human health [3,4]. Among synthetic dyes, azo dyes such as Congo red (CR) constitute approximately 70% of global dye production and are extensively utilized in textile, paper, and leather industries due to their favorable coloring properties [5]. The structural stability and complex aromatic composition of these dyes render them resistant to conventional biological degradation and hence leads to the development of efficient treatment technologies [6].

Various physicochemical and biological techniques have been employed for dye removal from industrial effluents, including chemical oxidation, membrane filtration, ion exchange, coagulation-flocculation, electrochemical treatment, photocatalytic degradation, and biological degradation [7,8]. While these methods demonstrate varying degrees of efficacy, many are associated with significant limitations such as high operational costs, energy intensity, generation of secondary pollutants, and complex maintenance requirements [9]. In contrast, adsorption has emerged as a preferred treatment strategy due to its operational simplicity, cost-effectiveness, high removal efficiency (typically 90–99%), minimal energy requirements, and potential for adsorbent regeneration [10]. The versatility of adsorption extends to the removal of diverse contaminants including heavy metals, organic compounds, and both cationic and anionic dyes [11]. Among various adsorbents used to treat effluent water, naturally available materials are most attractive nowadays, as they are abundant and cheaper to process. Laterite soil [12] is one of them and has the potential to adsorb dyes from wastewater.

The optimization of adsorption processes traditionally involves varying one factor at a time (OFAT), an approach that is labor-intensive, time-consuming, and incapable of detecting interaction effects between parameters [13]. Design of Experiments (DoE) offers a statistically robust alternative by enabling simultaneous evaluation of multiple factors and their interactions through structured experimental designs [14]. Response Surface Methodology (RSM), a collection of

IARJSET ISSN (O) 2393-8021, ISSN (P) 2394-1588

International Advanced Research Journal in Science, Engineering and Technology

Impact Factor 8.066 ⁜ Peer-reviewed & Refereed journal ⁜ Vol. 11, Issue 8, August 2024

DOI: 10.17148/IARJSET.2024.11842

mathematical and statistical techniques, facilitates the development of predictive models, identification of optimal conditions, and visualization of factor-response relationships through contour and surface plots [15]. Central Composite Design (CCD), a widely applied RSM approach, integrates factorial points, axial points, and center points to efficiently explore the experimental domain and fit quadratic models [16]. The application of RSM-CCD in adsorption studies significantly reduces experimental runs while providing comprehensive understanding of parameter interactions, making it an indispensable tool for process optimization in environmental engineering [17].

This study aims to evaluate the efficacy of treated laterite for Congo red dye removal and optimize the operational parameters using Response Surface Methodology with Central Composite Design. The specific objectives include: (i) investigating the individual effects of pH, contact time, initial concentration, dosage, and temperature on adsorption performance; (ii) developing a predictive model for dye removal efficiency; (iii) identifying significant factor interactions through ANOVA; and (iv) determining optimal conditions for maximum dye uptake.

2. MATERIALS AND METHODS

2.1 Materials and Instruments

Congo red dye (C.I. 22120, molecular formula $C_{32}H_{22}N_6Na_2O_6S_2$, molecular weight 696.66 g/mol) was procured from M/s Qualigens and used without further purification. A stock solution of 1000 mg/L was prepared by dissolving 1.0 g of dye in 1000 mL of distilled water. Working solutions of desired concentrations were prepared by serial dilution.

Raw Laterite is a naturally available material was procured from West Bengal, India. The powdered particles were sieved, and particles of size -140 mesh +170 mesh were collected, with an average size of 96.5 µm. The treated laterite was prepared from raw laterite using the procedure developed by maiti et al [18] . Acid treatment was to enhance to adsorption characteristics of laterite. All reagents used in this investigation were of A.R. grade. Double distilled water was used for preparing solutions throughout the study.

A digital pH meter (model number WTH-10, M/s Wensar, India) was used for all pH measurements. The absorbance measured on a UV/VIS spectrophotometer model number CE7400 (M/s Cecil, England) over a wavelength of 498 nm was used to estimate the concentration of the dye solutions.

2.2 Experimental Procedures

Effect of pH: A 25 mg/L Congo red solution was prepared, and the pH was adjusted to values ranging from 2 to 6 using dilute HCl (1N, 0.1N, 0.01N). Precipitation was observed at pH < 4; therefore, the operational range was established at pH 4–7 for subsequent studies. 50 ml of dye solution was contacted with 250 mg TL and agitated at 100 rpm for 120 minutes.

Effect of Contact Time: 30 mg/L solution was prepared at pH 5. Aliquots of 50 mL were contacted with 250 mg TL and agitated for predetermined intervals (1–120 minutes). Samples were withdrawn at specified time points, centrifuged, and analyzed spectrophotometrically.

Effect of Initial Concentration: Dye solutions ranging from 5 to 200 mg/L were prepared at pH 5. 50 ml of each solution was contacted with 250 mg TL for 90 minutes at 100 rpm.

Effect of Adsorbent Dosage: Dosages ranging from 50 to 1000 mg were added to 50 mL of 30 mg/L dye solution (pH 5) and agitated for 90 minutes.

Effect of Temperature: Adsorption experiments were conducted at varying temperatures (30–60°C) to study the thermal effect on removal efficiency.

Following agitation, samples were centrifuged at 6000 rpm for 10 minutes. The supernatant was analyzed using UV-Vis spectrophotometry, and percentage removal was calculated using Equation (1):

$$Removal\ (\%) = (C_o - C_e) / C_o \times 100$$

where C_o and C_e represent initial and equilibrium concentrations (mg/L), respectively. Dye uptake capacity (q_e, mg/g) was calculated using Equation (2):

$$q_e = (C_o - C_e) \times V / m$$

where V is the solution volume (L) and m is the adsorbent mass (g).

IARJSET

ISSN (O) 2393-8021, ISSN (P) 2394-1588

International Advanced Research Journal in Science, Engineering and Technology

Impact Factor 8.066 ⁜ Peer-reviewed & Refereed journal ⁜ Vol. 11, Issue 8, August 2024

DOI: 10.17148/IARJSET.2024.11842

2.3 Design of Experiments and Response Surface Methodology

Based on preliminary single-factor experiments, three parameters exhibiting significant influence on adsorption were selected for optimization: pH (4–7), initial dye concentration (10–50 mg/L), and adsorbent dosage (200–1500 mg). Contact time was fixed at the equilibrium time 90 minutes, and temperature was excluded due to negligible effect.

A Central Composite Face-Centered (CCF) design was employed within the RSM framework. The design comprised 20 experimental runs including 8 factorial points, 6 axial points, and 6 center points. The number of experiments was determined by $N = 2^k + 2k + N_0$, where k = 3 factors. Coded variables were assigned as −1 (low), 0 (center), and +1 (high) levels (Table 1).

TABLE 1. EXPERIMENTAL FACTORS AND LEVELS FOR CCD

Factor	Variable	−1 (Low)	0 (Center)	+1 (High)
X_1	pH	4	5.5	7
X_2	Concentration (mg/L)	10	30	50
X_3	Dosage (mg)	200	850	1500

A quadratic polynomial model was fitted to the experimental data:

$$Y = \beta_0 + \Sigma\beta_i X_i + \Sigma\beta_{ii} X_i^2 + \Sigma\Sigma\beta_{ij} X_i X_j + \varepsilon$$

where Y is the predicted response (% removal), β_0 is the intercept, β_i are linear coefficients, β_{ii} are quadratic coefficients, β_{ij} are interaction coefficients, and ε is the random error.

Analysis of Variance (ANOVA) was performed to evaluate model significance, factor effects, and interactions. Model adequacy was assessed using coefficient of determination (R^2), adjusted R^2, predicted R^2, and lack-of-fit test. Three-dimensional surface plots and contour plots were generated using python code and origin software (trail version) to visualize response surfaces and identify optimal regions. All statistical analyses and optimizations were conducted using Design-Expert software (trail version).

3. RESULTS AND DISCUSSION

3.1 Individual Parameter Studies

3.1.1 Effect of pH

The pH study from Fig. 1 revealed that removal of Congo red is maximum in acidic medium and removal efficiency decreases in basic medium. This trend is attributed to the protonation of TL surface functional groups under acidic conditions, generating positive surface charge that enhances electrostatic attraction toward the anionic sulfonate groups of Congo red dye [19]. At pH values below 4, precipitation phenomena was observed, likely due to dye aggregation or acid-induced structural changes. Hence, the operational pH range of 4–7 was established for subsequent CCD experiments.

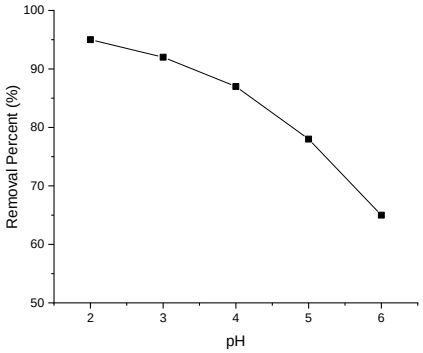

Fig. 1. Effect of pH (Conditions: 25 mg/L, 250 mg adsorbent, 120 min, 100 rpm).

3.1.2 Effect of Contact Time

From Fig. 2, It was observed that approximately 80% of total dye removal occurred within the first 30 minutes, suggesting vacant active sites on the fresh adsorbent surface are abundant. The removal rate progressively decreased as

IARJSET
ISSN (O) 2393-8021, ISSN (P) 2394-1588
International Advanced Research Journal in Science, Engineering and Technology
Impact Factor 8.066 ⁜ Peer-reviewed & Refereed journal ⁜ Vol. 11, Issue 8, August 2024
DOI: 10.17148/IARJSET.2024.11842

sites became occupied, with equilibrium established at 90 minutes. Beyond this point, no significant change in removal efficiency was observed, indicating saturation of available binding sites [20].

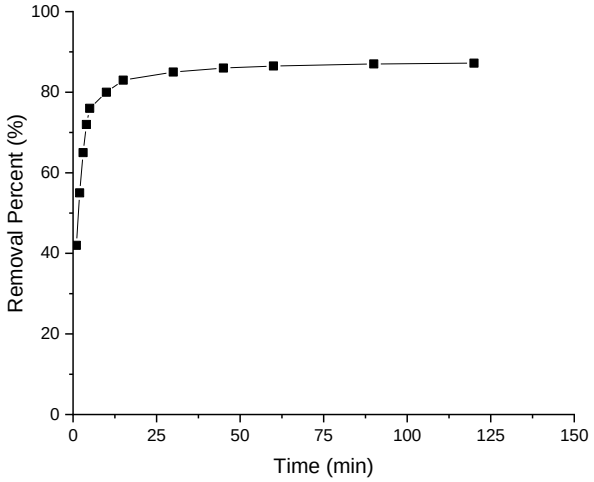

Fig. 2. Effect of contact time at 30 mg/L (Conditions: pH 5, 250 mg adsorbent, 100 rpm).

3.1.3 Effect of Initial Dye Concentration

At lower concentrations (5–20 mg/L), high percentage removal (>90%) was achieved due to favorable adsorbent-to-adsorbate ratios. As concentration increased to 50–200 mg/L, percentage removal decreased while the dye uptake (mg/g) increased as shown in Fig. 3. The enhanced driving force at higher concentrations facilitates greater diffusion of dye molecules to adsorbent surfaces, though site saturation limits proportional removal efficiency [21].

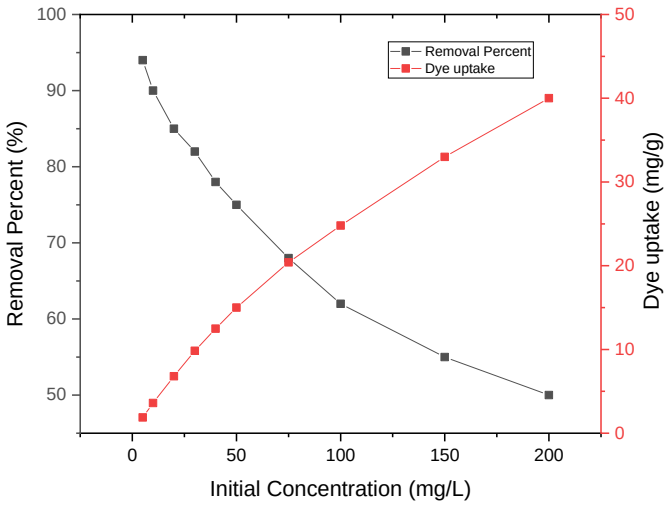

Fig. 3. Effect of initial dye concentration (Conditions: pH 5, 250 mg adsorbent, 90 min, 100 rpm).

3.1.4 Effect of Adsorbent Dosage

As shown in Fig. 5, Increasing dosage from 50 to 1000 mg resulted in improved percentage removal due to increased availability of active binding sites as shown in Fig. 4. However, dye uptake per unit mass (mg/g) exhibited an inverse relationship with dosage, suggesting underutilization of surface area and potential particle aggregation at higher adsorbent loadings [22]. The optimal dosage range was identified as 200–1500 mg for CCD optimization.

IARJSET
ISSN (O) 2393-8021, ISSN (P) 2394-1588
International Advanced Research Journal in Science, Engineering and Technology
Impact Factor 8.066 ⁜ Peer-reviewed & Refereed journal ⁜ Vol. 11, Issue 8, August 2024
DOI: 10.17148/IARJSET.2024.11842

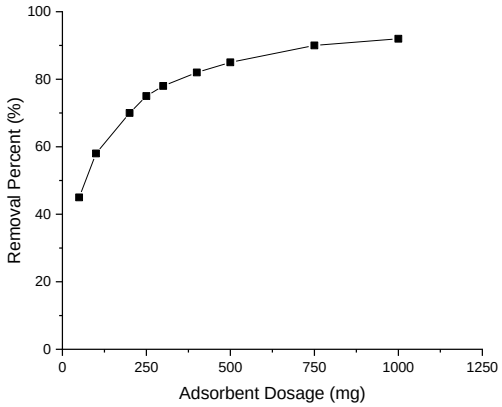

Fig. 4. Effect of adsorbent dosage (Conditions: 30 mg/L, pH 5, 90 min, 100 rpm).

3.1.5 Effect of Temperature

Temperature variation (30–60°C) demonstrated negligible influence on removal percentage, suggesting that the adsorption process is not thermally activated within this range. This observation simplifies process design by eliminating the need for temperature control systems, thereby reducing operational costs [23].

3.2 Response Surface Methodology Results

3.2.1 Experimental Design and Model Fitting

The CCF design matrix and corresponding experimental responses are presented in Table 2. The design encompassed 20 runs with varying combinations of pH, concentration, and dosage.

TABLE 2. CENTRAL COMPOSITE DESIGN MATRIX AND EXPERIMENTAL RESPONSES

Run	pH (X_1)	Conc. (X_2)	Dosage (X_3)	Dye Uptake (mg/g)	% Removal
1	4	10	200	1.332	53.29
2	7	10	200	0.592	23.70
3	4	50	200	3.256	26.05
4	7	50	200	1.654	13.23
5	4	10	1500	0.313	93.89
6	7	10	1500	0.316	94.86
7	4	50	1500	1.575	94.52
8	7	50	1500	1.345	80.73
9	4	30	850	1.539	87.20
10	7	30	850	1.146	64.95
11	5.5	10	850	0.545	92.66
12	5.5	50	850	1.931	65.66
13	5.5	30	200	1.582	21.09
14	5.5	30	1500	0.961	96.09
15	5.5	30	850	1.460	82.72
16	5.5	30	850	1.461	82.80
17	5.5	30	850	1.512	85.65
18	5.5	30	850	1.359	77.01
19	5.5	30	850	1.497	84.84
20	5.5	30	850	1.517	85.98

The regression equation for percentage removal in uncoded units was:

$$\%Removal = 37.3 + 3.7(pH) - 0.718(Conc) + 0.1023(Dosage) - 1.13(pH)^2 + 0.00139(Conc)^2 - 0.000047(Dosage)^2 + 0.0084(pH \times Conc) + 0.00379(pH \times Dosage) + 0.000233(Conc \times Dosage)$$

ISSN (O) 2393-8021, ISSN (P) 2394-1588

IARJSET

International Advanced Research Journal in Science, Engineering and Technology

Impact Factor 8.066 ⁜ Peer-reviewed & Refereed journal ⁜ Vol. 11, Issue 8, August 2024

DOI: 10.17148/IARJSET.2024.11842

3.2.2 Model Summary and Adequacy

The model summary statistics are presented in Table 3.

TABLE 3. MODEL SUMMARY STATISTICS

S	R^2	Adjusted R^2	Predicted R^2
6.5235	97.07%	94.42%	67.98%

The high R^2 value (0.9707) indicates that 97.07% of variability in removal efficiency is explained by the model. The adjusted R^2 (0.9442) accounts for the number of predictors and confirms excellent model fit. The moderate predicted R^2 (0.6798) suggests reasonable predictive capability for interpolation within the design space as shown in the model validation plot (Fig. 5).

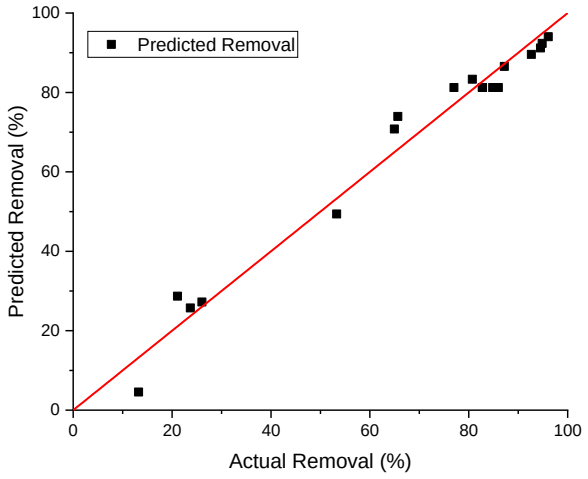

Fig. 5. Predicted versus actual values for dye removal percentage (Model validation plot).

3.2.3 Analysis of Variance

ANOVA results (Table 4) and Pareto Chart (Fig. 6) demonstrate that the overall model is highly significant ($F = 49.44$, $p < 0.0001$). The linear terms of all three factors were statistically significant: concentration exhibited the strongest effect ($F = 256.94$, $p < 0.0001$), followed by dosage ($F = 88.26$, $p < 0.0001$) and pH ($F = 50.75$, $p < 0.0001$). Among interaction terms, pH × dosage was highly significant ($F = 32.36$, $p = 0.0002$), while pH × concentration showed moderate significance ($F = 8.64$, $p = 0.015$). The concentration × dosage interaction was not statistically significant ($p = 0.092$). Quadratic terms were collectively non-significant ($p = 0.272$), suggesting predominantly linear relationships within the experimental domain.

TABLE 4. ANOVA RESULTS FOR PERCENTAGE REMOVAL

Source	DF	Adj SS	Adj MS	F-Value	P-Value
Model	9	7.688	0.854	49.44	<0.0001
Linear	3	6.841	2.280	131.98	<0.0001
pH	1	0.877	0.877	50.75	<0.0001
Concentration	1	4.439	4.439	256.94	<0.0001
Dosage	1	1.525	1.525	88.26	<0.0001
Square	3	0.078	0.026	1.51	0.272
pH^2	1	0.001	0.001	0.03	0.868
$Conc^2$	1	0.023	0.023	1.31	0.279
$Dosage^2$	1	0.009	0.009	0.53	0.483
2-Way Interaction	3	0.769	0.256	14.84	0.001
pH × Conc	1	0.150	0.150	8.64	0.015
pH × Dosage	1	0.559	0.559	32.36	0.000

ISSN (O) 2393-8021, ISSN (P) 2394-1588

IARJSET

International Advanced Research Journal in Science, Engineering and Technology

Impact Factor 8.066 ⁜ Peer-reviewed & Refereed journal ⁜ Vol. 11, Issue 8, August 2024

DOI: 10.17148/IARJSET.2024.11842

Conc × Dosage	1	0.060	0.060	3.48	0.092
Error	10	0.173	0.017		
Lack-of-Fit	5	0.156	0.031	9.07	0.015
Pure Error	5	0.017	0.003		
Total	19	7.861			

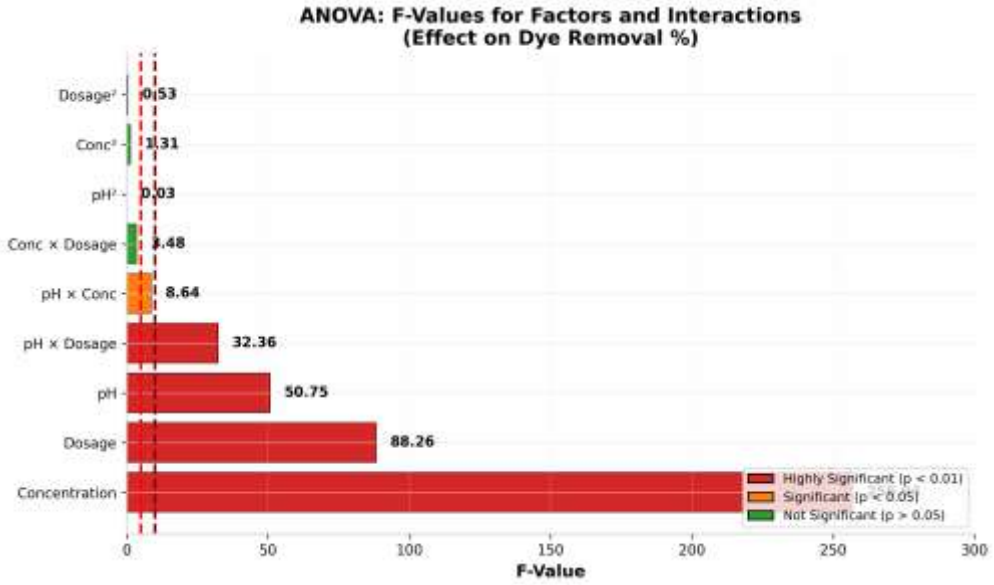

Fig. 6. Pareto chart showing F-values for factors and interactions affecting dye removal (Red: highly significant $p < 0.01$; Orange: significant $p < 0.05$; Green: not significant $p > 0.05$).

3.2.4 Response Surface Analysis

Three-dimensional surface plots were generated to visualize the interactive effects of factors on dye removal efficiency. The surface plot of dye uptake versus pH and concentration (Fig. 7a) revealed significant interaction effects, evidenced by the sloping curvature of the response surface. At low pH and low concentration, moderate removal was observed; however, the combination of low pH with high concentration resulted in substantially increased dye uptake. This synergistic interaction confirms that acidic conditions enhance the adsorption capacity even at elevated dye loadings [24].

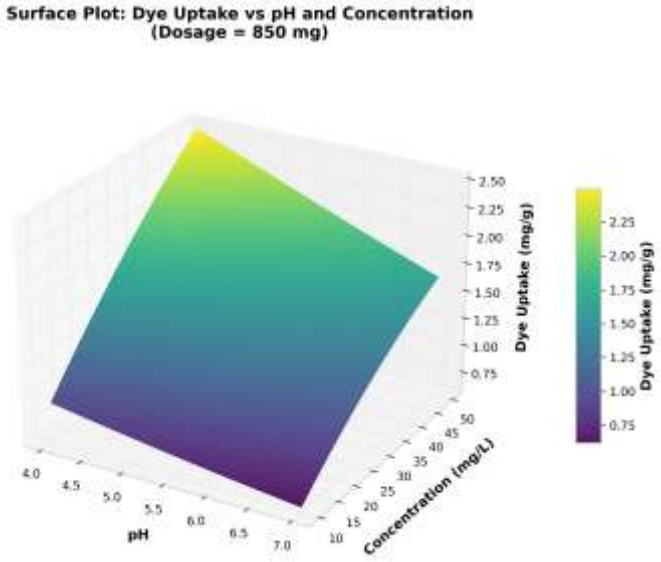

Fig. 7. (a) Three-dimensional surface plot showing dye uptake as a function of pH and concentration at fixed dosage (850 mg).

IARJSET

ISSN (O) 2393-8021, ISSN (P) 2394-1588

International Advanced Research Journal in Science, Engineering and Technology

Impact Factor 8.066 ⁜ Peer-reviewed & Refereed journal ⁜ Vol. 11, Issue 8, August 2024

DOI: 10.17148/IARJSET.2024.11842

The pH versus dosage interaction surface plot (Fig. 7b) exhibited the most pronounced curvature, with high removal efficiencies concentrated in specific regions of the design space. Maximum removal (>95%) was achieved at low pH combined with high dosage, while high pH values consistently produced lower efficiencies regardless of dosage. The steep gradient along the pH axis at constant dosage values confirms the dominant role of pH in controlling adsorption performance [25].

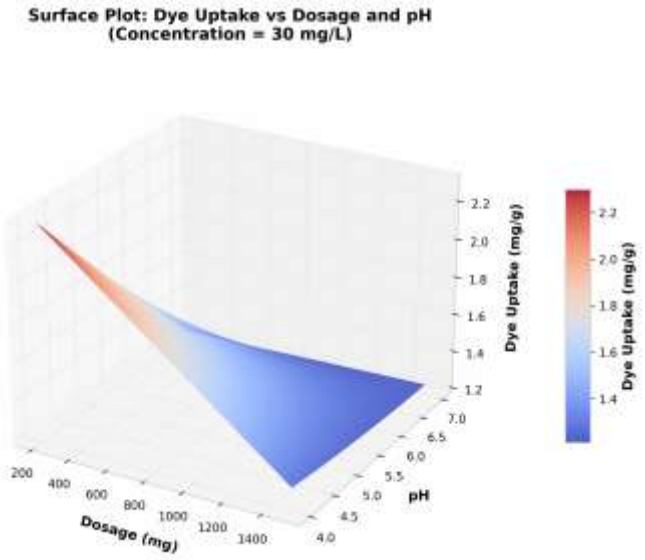

Fig. 7. (b) Three-dimensional surface plot showing dye uptake as a function of dosage and pH at fixed concentration (30 mg/L).

The concentration versus dosage interaction surface (Fig. 7c) displayed relatively flat topology with gradual transitions, consistent with the non-significant p-value (0.092) for this interaction term. While individual effects of both concentration and dosage were significant, their combined influence did not produce synergistic or antagonistic effects beyond additive contributions [26].

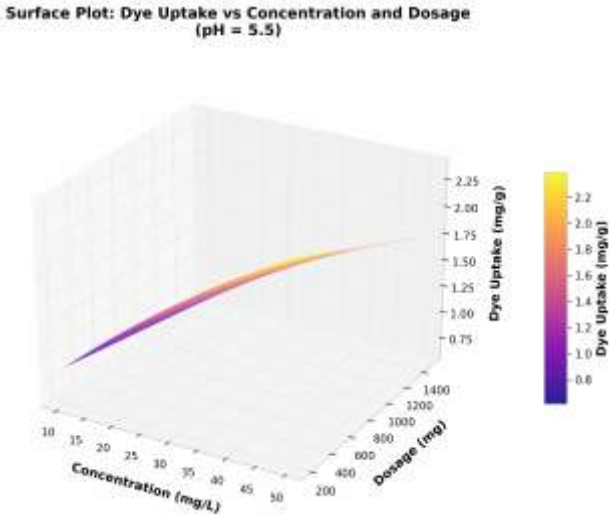

Fig. 7. (c) Three-dimensional surface plot showing dye uptake as a function of concentration and dosage at fixed pH (5.5).

3.2.5 Contour Plots

Two-dimensional contour plots were generated to identify optimal operating regions within the design space.

The contour plot of percentage removal versus pH and concentration (Fig. 8a) revealed significant interaction effects, with the sloping contour lines indicating that changes in both parameters simultaneously produce non-linear responses.

IARJSET

ISSN (O) 2393-8021, ISSN (P) 2394-1588

International Advanced Research Journal in Science, Engineering and Technology

Impact Factor 8.066 ⁜ Peer-reviewed & Refereed journal ⁜ Vol. 11, Issue 8, August 2024

DOI: 10.17148/IARJSET.2024.11842

The optimal region (green zone, >90% removal) was concentrated at lower pH values (4.0–5.0) across the concentration range, with the highest efficiencies observed at pH 4.8 and concentration 52 mg/L.

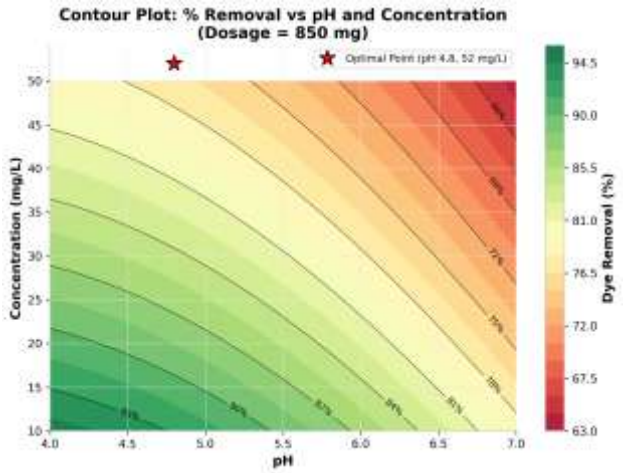

Fig. 8. (a) Contour plot showing percentage removal as a function of pH and concentration at fixed dosage (850 mg). The red star indicates the optimal point.

The pH versus dosage contour plot (Fig. 8b) exhibited the most pronounced interaction, with tightly spaced contour lines indicating steep response gradients. Maximum removal efficiencies (>95%) were achieved in the region of low pH (4.0–5.0) combined with high dosage (>1000 mg), while high pH values consistently produced poor removal regardless of dosage. The optimal point (pH 4.8, dosage 850 mg) lies within the high-efficiency zone, confirming the robustness of the optimization.

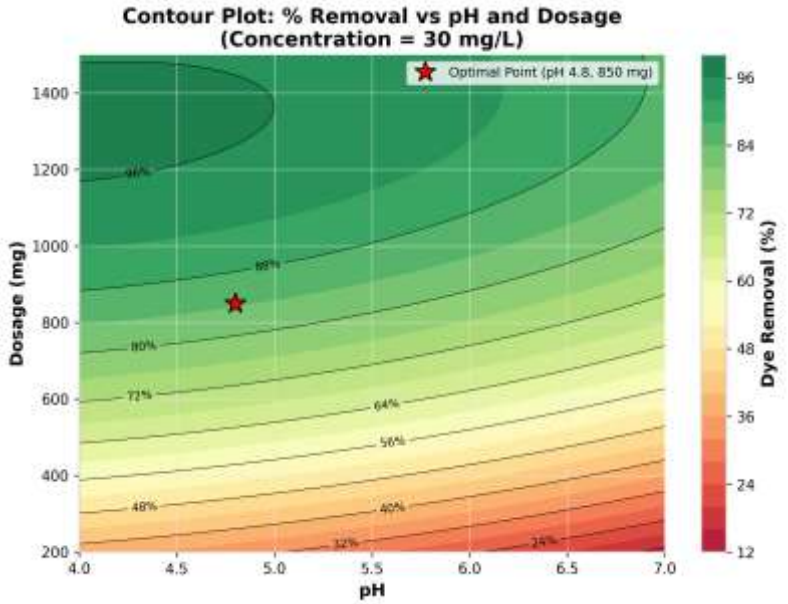

Fig.8. (b) Contour plot showing percentage removal as a function of pH and dosage at fixed concentration (30 mg/L). The red star indicates the optimal point.

3.3 Optimization

Numerical optimization was performed to maximize percentage removal within the experimental constraints. The optimal conditions were determined as: pH 4.8, initial dye concentration 52 mg/L, and adsorbent dosage 850 mg. Under these conditions, the predicted removal efficiency was approximately 96% with high desirability. The proximity of optimal pH to the lower boundary confirms the importance of acidic conditions for anionic dye adsorption on treated laterite.

IARJSET ISSN (O) 2393-8021, ISSN (P) 2394-1588

International Advanced Research Journal in Science, Engineering and Technology

Impact Factor 8.066 ⁜ Peer-reviewed & Refereed journal ⁜ Vol. 11, Issue 8, August 2024

DOI: 10.17148/IARJSET.2024.11842

4. CONCLUSION

This study successfully demonstrated the application of treated laterite as an effective, low-cost adsorbent for the removal of Congo red dye from aqueous solutions. Individual parameter studies established an equilibrium contact time of 90 minutes and confirmed negligible temperature effects, simplifying process design requirements. The Central Composite Design-based Response Surface Methodology provided a statistically robust framework for optimizing operational parameters with minimal experimental runs.

ANOVA analysis confirmed that all three investigated factors—pH, initial dye concentration, and adsorbent dosage—significantly influenced dye removal efficiency, with initial concentration exhibiting the dominant effect. Significant two-way interactions between pH and dosage, and between pH and concentration, underscore the importance of considering combined parameter effects rather than isolated variations. The quadratic model achieved excellent fit ($R^2 = 0.9707$, adjusted $R^2 = 0.9442$) and reliable predictive capability.

The optimized conditions (pH 4.8, concentration 52 mg/L, dosage 850 mg) yielded maximum dye removal efficiency of approximately 96%. These results establish treated laterite as a promising sustainable adsorbent for textile wastewater treatment applications. Future research should investigate adsorption isotherm and kinetic modeling, regeneration studies for adsorbent reuse, and application to real textile effluents containing dye mixtures and auxiliary chemicals.

REFERENCES

[1] Islam MR, Mostafa MG. Textile dyeing effluents and environment concerns—a review. J Environ Sci Nat Resour. 2018;11(1-2):131-144. DOI: https://doi.org/10.3329/jesnr.v11i1-2.43380.

[2] Van Pham T, Tran TV, Nguyen TD, et al. Development of response surface methodology for optimization of congo red adsorption utilizing exfoliated graphite as an efficient adsorbent. Mater Today Proc. 2020;22(4):2341-2350. DOI: https://doi.org/10.1016/j.matpr.2020.03.356.

[3] Taufik R, Mohamad M, Wannahari R, et al. Spent coffee ground as low-cost adsorbent for congo red dye removal from aqueous solution. IOP Conf Ser Earth Environ Sci. 2021;765(1):012089. DOI: 10.1088/1755-1315/765/1/012089.

[4] Ponnusamy SK, Subramaniam R. Process optimization studies of Congo red dye adsorption onto cashew nut shell using response surface methodology. Int J Ind Chem. 2013;4(17):1-10. DOI: https://doi.org/10.1186/2228-5547-4-17.

[5] Asfaram A, Ghaedi M, Dashtian K. Ultrasound assisted combined molecularly imprinted polymer for selective extraction of nicotinamide in human urine and milk samples: Spectrophotometric determination and optimization study. Ultrason Sonochem. 2017;34:640-650. DOI: https://doi.org/10.1016/j.ultsonch.2016.06.018.

[6] Essekri A, Aarab N, Laabd M, et al. Enhanced adsorptive removal of crystal violet dye from aqueous media using citric acid modified red- seaweed: experimental study combined with RSM process optimization. J Disp Sci Technol. 2022;43(9):1359-1372. DOI: https://doi.org/10.1080/01932691.2020.1857263.

[7] Laksaci H, Khelifi A, Belhamdi B, Trari M. The use of prepared activated carbon as adsorbent for the removal of orange G from aqueous solution. Microchem J. 2019;145:908-913. DOI: https://doi.org/10.1016/j.microc.2018.12.001.

[8] Navaei A, Yazdani M, Alidadi H, et al. Biosorption of Reactive Red 120 dye from aqueous solution using Saccharomyces cerevisiae: RSM analysis, isotherms and kinetic studies. Desalin Water Treat. 2019;171:418-427. DOI: https://doi.org/10.5004/dwt.2019.24780.

[9] Omokpariola DO, Otuosorochi JN. Batch adsorption studies on rice husk with methyl violet dye. World News Nat Sci. 2020;33:48-63. DOI: https://doi.org/10.5281/zenodo.18630260.

[10] Foo KY, Hameed BH. Insights into the modeling of adsorption isotherm systems. Chem Eng J. 2010;156(1):2-10. DOI: https://doi.org/10.1016/j.cej.2009.09.013.

[11] Crini G. Non-conventional low-cost adsorbents for dye removal: A review. Bioresour Technol. 2006;97(9):1061-1085. DOI: https://doi.org/10.1016/j.biortech.2005.05.001.

[12] Rani KS, Sarma GVS, Naidu KG, Ramesh KV, Adsorptive removal of chromium by modified laterite, in: Mater. Today Proc., Elsevier Ltd., 18(7), pp. 4882–4892 (2019). DOI: https://doi.org/10.1016/j.matpr.2019.07.479.

[13] Montgomery DC. Design and Analysis of Experiments. 10th ed. Hoboken: John Wiley & Sons; 2019. ISBN 978-1118-14692-7. DOI: https://doi.org/10.1016/j.matpr.2019.07.479.

[14] Box GEP, Wilson KB. On the experimental attainment of optimum conditions. J R Stat Soc Ser B. 1951;13(1):1-45.

IARJSET ISSN (O) 2393-8021, ISSN (P) 2394-1588

International Advanced Research Journal in Science, Engineering and Technology

Impact Factor 8.066 ⁜ Peer-reviewed & Refereed journal ⁜ Vol. 11, Issue 8, August 2024

DOI: 10.17148/IARJSET.2024.11842

[15] Myers RH, Montgomery DC, Anderson-Cook CM. Response Surface Methodology: Process and Product Optimization Using Designed Experiments. 4th ed. Hoboken: John Wiley & Sons; 2016. ISBN: 978-1-118-91601-8.

[16] Khuri AI, Mukhopadhyay S. Response surface methodology. Wiley Interdiscip Rev Comput Stat. 2010;2(2):128-149. DOI: https://doi.org/10.1002/wics.73.

[17] Bezerra MA, Santelli RE, Oliveira EP, Villar LS, Escaleira LA. Response surface methodology (RSM) as a tool for optimization in analytical chemistry. Talanta. 2008;76(5):965-977.
DOI: https://doi.org/10.1016/j.talanta.2008.05.019.

[18] Maiti A, Basu JK, De S. Development of a Treated Laterite for Arsenic Adsorption: Effect of Treatment Parameters. Ind Eng Chem Res. 2010; 49(10): 4873-4886. DOI: https://doi.org/10.1021/IE100612U.

[19] Salleh MAM, Mahmoud DK, Karim WAWA, Idris A. Cationic and anionic dye adsorption by agricultural solid wastes: A comprehensive review. Desalination. 2011;280(1-3):1-13. DOI: https://doi.org/10.1016/j.desal.2011.07.019.

[20] Worch E. Adsorption Technology in Water Treatment: Fundamentals, Processes, and Modeling. Berlin: De Gruyter; 2012. ISBN 978-3-11-024022-1.

[21] Ruthven DM. Principles of Adsorption and Adsorption Processes. New York: John Wiley & Sons; 1984. ISBN 0-471-86606-7.

[22] McKay G, Otterburn MS, Sweeney AG. The removal of colour from effluent using various adsorbents—III. Silica: Rate processes. Water Res. 1980;14(1):15-20. DOI: https://doi.org/10.1016/0043-1354(80)90037-8.

[23] Al-Degs YS, El-Barghouthi MI, El-Sheikh AH, Walker GM. Effect of solution pH, ionic strength, and temperature on adsorption behavior of reactive dyes on activated carbon. Dyes Pigm. 2008;77(1):16-23. DOI: https://doi.org/10.1016/j.dyepig.2007.03.001.

[24] Subramani SE, Thinakaran N. Isotherm, kinetic and thermodynamic studies on the adsorption behaviour of textile dyes onto chitosan. Process Saf Environ Prot. 2017;106:1-10. DOI: https://doi.org/10.1016/j.psep.2016.11.024.

[25] Kannan N, Sundaram MM. Kinetics and mechanism of removal of methylene blue by adsorption on various carbons—a comparative study. Dyes Pigm. 2001;51(1):25-40. DOI: https://doi.org/10.1016/S0143-7208(01)00056-0.

[26] Hamdaoui O. Batch study of liquid-phase adsorption of methylene blue using cedar sawdust and crushed brick. J Hazard Mater. 2006;135(1-3):264-273. DOI: https://doi.org/10.1016/j.jhazmat.2005.11.062.

